

Wide-Angle Triangulation Array Study of Simultaneous Primary Microseism Sources

ROBERT K. CESSARO AND W. WINSTON CHAN

Teddyne Geotech Alexandria Laboratory, Alexandria, Virginia

Persistent low frequency noise between 10 and 200 mHz due to storm systems is commonly observed as microseisms on seismic records from land and ocean bottom detectors. We report on an analysis of 20-second microseisms recorded simultaneously on two land-based long-period arrays (the Alaskan Long Period Array and the Large Aperture Seismic Array) during November 1973. Azimuths of approach are determined by applying frequency wave-number analysis and beam-forming techniques to coherent bandpass-filtered samples of the microseismic noise field recorded by the arrays. Microseismic source azimuths exhibit sufficient stability over periods of one hour to permit determination of reliable source locations by triangulation with the two arrays. Locations for two microseism noise sources associated with two separate Atlantic and Pacific pelagic storms were found simultaneously with these methods. In both cases, the microseismic noise source appears to be associated with nearshore processes. Although the gross spectral character of the microseisms displays the commonly observed primary- and double-frequency microseism peaks, slight spectral differences are apparent for the two noise sources.

INTRODUCTION

This paper presents results of a study of microseisms at approximately 50 mHz, generated by separate major oceanic storms located in the North Atlantic and North Pacific oceans. These microseismic signals were recorded on the Alaskan Long Period Array (ALPA) and the Large Aperture Seismic Array (LASA) in Montana during November 26-28, 1973. Array analyses of microseisms have proven to be very effective in providing detailed information on the source generation and propagation modes of microseisms [Capon, 1970; Haubrich and McCamy, 1969; Toksöz and Lacoss, 1968]. In this study, we apply high-resolution frequency wave-number (FK) analysis and beam-forming techniques to the array data to determine direction of approach for microseisms arriving as surface waves from pelagic storms recorded at each array. We perform a wide aperture triangulation from simultaneous observations made at the ALPA and LASA arrays, adding to the work of previous array studies [Toksöz and Lacoss, 1968; Lacoss, et al., 1969; Capon, 1969, 1970] by improving the resolution of distance and azimuth between sources and receivers. The information on distance is most important since we may then address the question of near-coast or near-source origin of the ambient noise field. We believe this is the first simultaneous determination of multiple microseismic source locations with this method.

Microseisms are typically long-period surface waves identified by Haubrich et al. [1963] as primary- and double-frequency microseisms, covering two distinctly different frequency bands: 80 mHz and 150 mHz, respectively. The primary microseisms are observed on land between 40 and 80 mHz as reported by Oliver [1962], Haubrich et al. [1963], and Darbyshire and Okeke [1969]. These waves have a spectral peak equal to the wavelengths of the dominant ocean waves and appear to form in shallow water by the interaction of ocean swells with a shoaling ocean bottom having appreciable depth variation [e.g., Oliver, 1962]. The double-frequency microseisms with dominant periods between 6 and 10 seconds (100-160 mHz) have been observed on land by Darbyshire [1950], Iyer [1958], and Hasselmann [1963]. Longuet-Higgins [1950] proposed that the double-frequency microseisms are the consequence of an in-

terplay amongst ocean waves of equal frequency traveling in opposite directions and resulting in a nonlinear, second-order pressure perturbation on the ocean bottom. In a study of double-frequency microseisms recorded at LASA, Haubrich and McCamy [1969] concluded that coastal reflection of ocean waves is the principal agency responsible for their generation.

Using data from large aperture seismic arrays offers potentially higher resolution in the study of microseism directionality and source location than that obtainable from single station or network data. But for various reasons, array data are not easy to acquire and have not been fully utilized. Haubrich and McCamy [1969] and Toksöz and Lacoss [1968] studied frequency wave-number spectra of microseism recordings at LASA, providing detailed observations about microseismic sources and propagation modes. Numerous investigations of microseisms have yielded valuable information directed towards an understanding of their generation and propagation. Yet, disparities remain in the observations, and theoretical questions remain unresolved. Contradictions persist regarding the generation of microseisms observed on land. Whether they are near-coast effects [e.g., Haubrich and McCamy, 1969] or due to distant source [e.g., Iyer, 1958] remains unresolved. The effects of path propagation of microseisms are still little understood, and the generation of Love wave energy [Rind and Donn, 1979] in microseisms awaits further investigations.

DATA DESCRIPTION

The low-frequency microseism signals were obtained from digitized recordings collected by both the LASA and ALPA arrays during the period November 26-28, 1973. Both arrays recorded digitally at 1-Hz sampling frequency. The frequency response of the long-period elements of both arrays is flat to velocity from 25- to 200-second period (5-40 mHz). The location and pattern of each array are shown in Figure 1. Differences in the array dimensions and geometries are reflected in the resolution observed in the analysis of their respective data.

The LASA array, operating from 1965 through 1978, was composed of 21 subarrays, each containing 25 vertical high-frequency (1 Hz) seismometers. In addition, one vertical and two horizontal long-period (25-s) seismometers are located in the centers of each subarray and provide the data for this study. The horizontal seismometers are installed with their sensitive axes oriented north and east. Additional details on LASA instrumentation are given by Forbes et al. [1965].

Copyright 1989 by The American Geophysical Union.

Paper number 89JB01218.
0148-0227/89/89JB-01218\$05.00

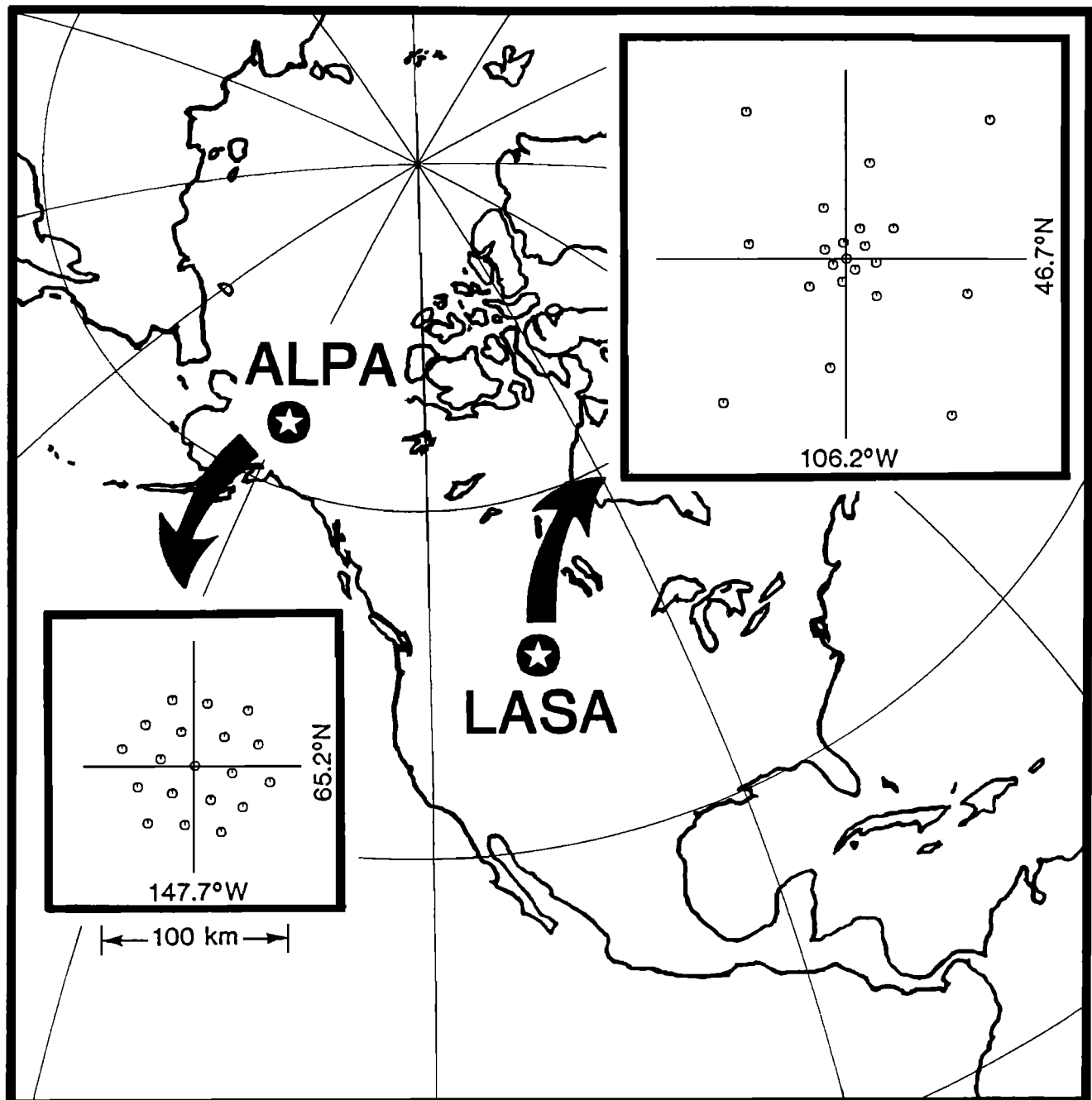


Fig. 1. Map showing locations of ALPA and LASA arrays. Array configurations are shown at a common scale in the map inserts.

The ALPA array, operating from 1970 through 1982, was composed of 19 long-period triaxial seismometers. The individual long-period seismometer modules recorded three orthogonal axes of sensitivity, oriented 120° apart (in map view), starting from 60° east of true north and inclined $35^\circ 56'$ above horizontal. Prior to analysis, the component signals are mathematically rotated to obtain vertical and horizontal signals. We have high confidence that the rotated signals accurately reflect ground motion because the components are well matched in both frequency and phase response [Geotech, 1970].

In this paper we analyze microseisms recorded during the peak activity of two widely separated storm systems. The storms were selected from the *Mariners Weather Log* [1973] by examining the

log for the presence of isolated principal cyclone tracks occurring simultaneously in the North Atlantic and the North Pacific oceans while both arrays were in full operation. The selected storms occurred during the time period November 22-28, 1973. Representative examples of the microseisms recorded on both arrays, shown in Figure 2, indicate the data quality and coherence across the arrays. The spatial coherence of long-period surface waves propagating across both arrays has been previously analyzed [Mack, 1972] and so will not be discussed here. In order to permit adequate detection and resolution by FK analysis, the amplitudes of the microseisms chosen for analysis must remain sufficiently above the noise levels generated by other local and global sources recorded at both arrays.

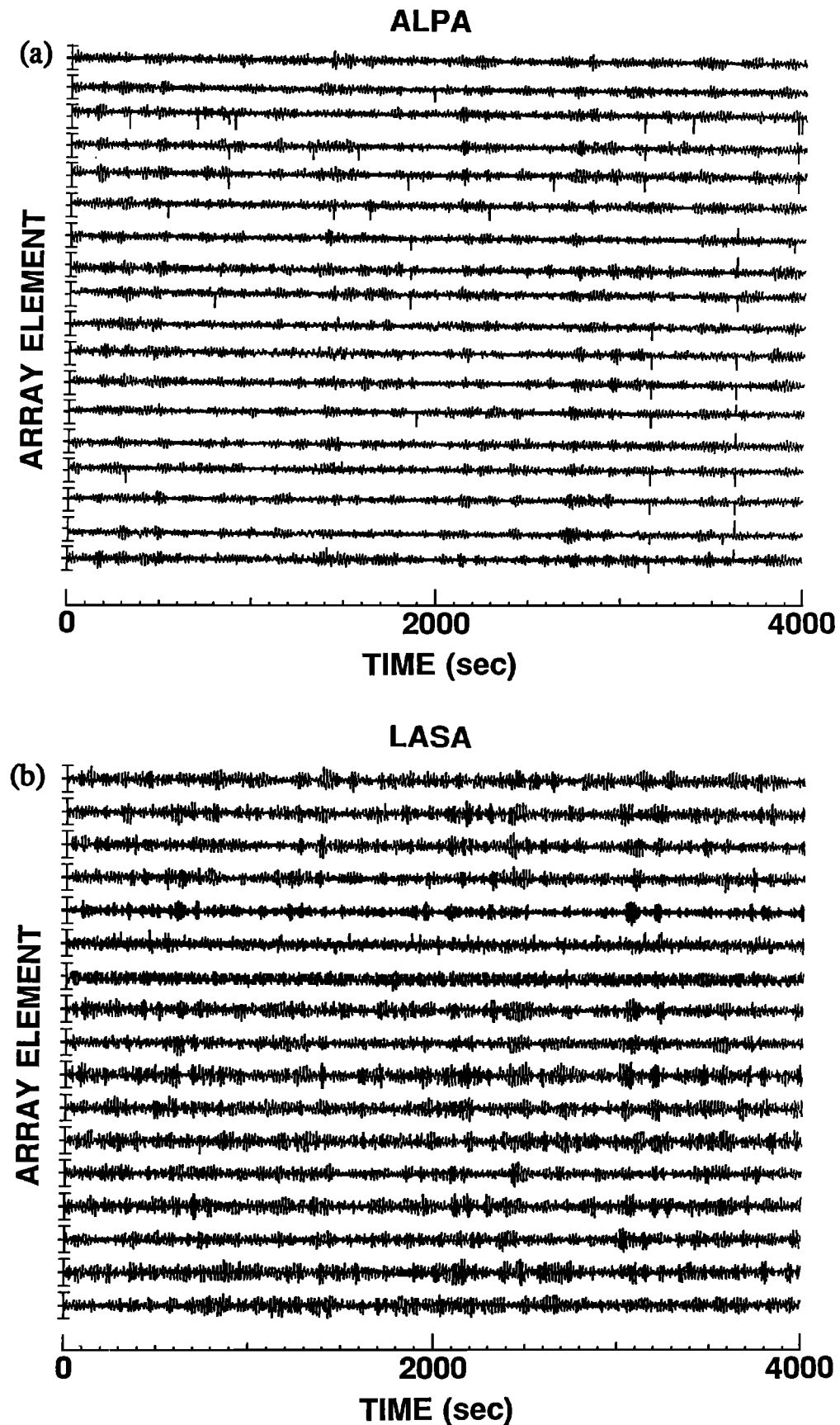


Fig. 2. Examples of microseism signals recorded on (a) 18 elements of ALPA and (b) 17 elements of LASA arrays.

Microseisms from several pelagic storms were analyzed in the course of this study but were discarded due to low signal amplitudes or instrument malfunction.

METHODS OF ANALYSIS

FK Analysis

Frequency wave-number power spectra provide an excellent means for discriminating the seismic noise field by phase velocity and direction of approach. We use the high-resolution FK method described by *Capon* [1969]. This method differs from the conventional FK method in that the wave-number window shape preserves a unity response for each frequency wave-number power estimate sought, thus enhancing the wave-number resolution. Digitized samples of microseism data for successive time windows were subjected to frequency wave-number analysis to determine directions of approach and phase velocities and to examine the temporal variation in FK power spectra [*Capon*, 1969, 1970; *Haubrich and McCamy*, 1969]. Figure 3 shows a sample result of the FK processing. The contours shown represent 1 dB increments in power referred to the peak power at a given frequency. The phase velocity determined lies within the range of Rayleigh waves propagating over continental paths.

We chose the microseism records to coincide approximately with the peak activity of two major storms located in the North Pacific and North Atlantic oceans beginning at 0600 UT, November 26, and running to 1800 UT, November 28, 1973. Analysis was performed on continuous 4000-second signal samples excerpted at 6-hour intervals from the data archives. We used vertical component signals

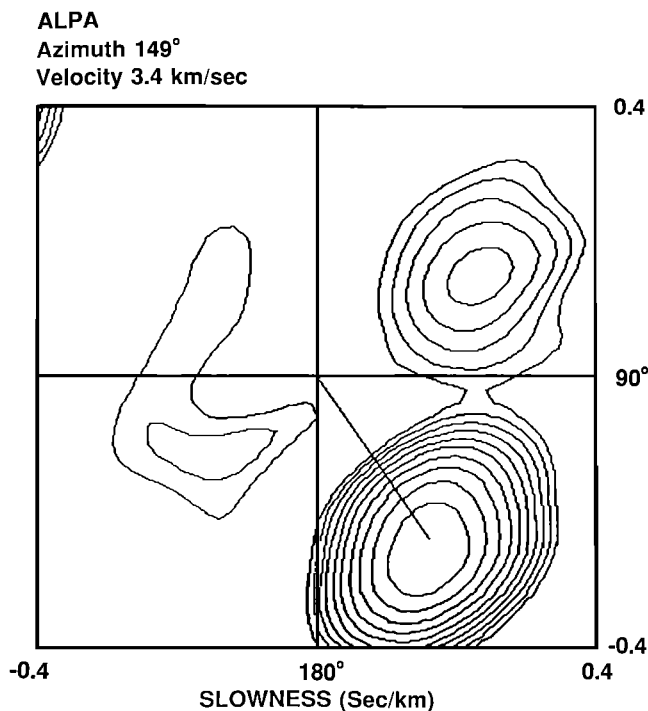


Fig. 3a. An example of frequency wave-number processing for microseisms recorded at ALPA at 50 mHz (20 s). The power peak in the southeast quadrant indicates a direction of approach to ALPA from about 149° with a phase velocity of about 3.4 km/s. This microseismic source is identified with a storm located in the North Pacific basin. The contours are drawn at 1-dB intervals referred to the peak power at this frequency. Also note the large peak in the northeast quadrant. This represents a second microseism source associated with a North Atlantic storm.

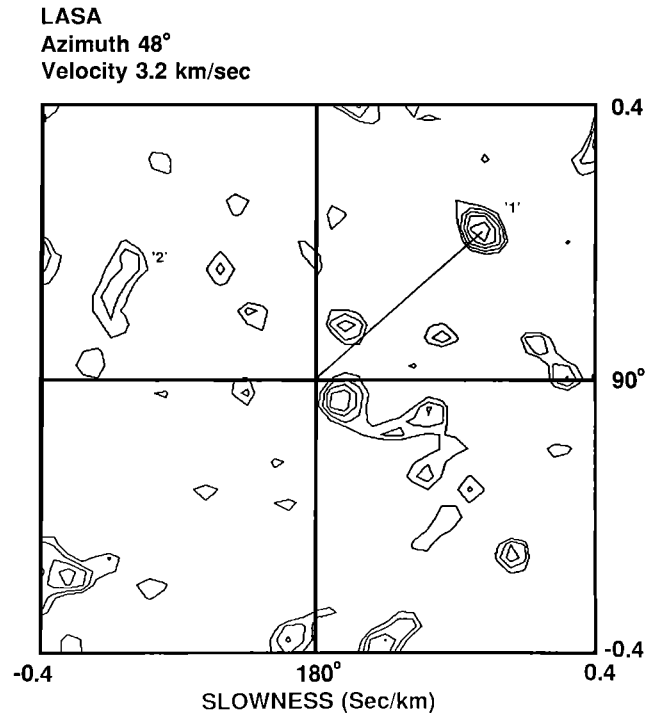


Fig. 3b. An example of frequency-wave number processing for microseisms recorded at LASA at 50 mHz (20 s). Power peak '1' in the northeast quadrant indicates a direction of approach to LASA from about 48° with a phase velocity of about 3.2 km/s. This microseismic source is identified with a storm located in the North Atlantic. The contours are drawn at 1-dB intervals and refer to the peak power at this frequency. Also note the presence of other peaks. Peak '2' in the northwest quadrant, though not prominent during this time window, fluctuates in relative power compared with peak '1'. By using a running window FK analysis, both power peaks may contribute to potential source locations. Peak '2' is identified with a storm in the North Pacific basin. The high phase velocity peak in the southeast quadrant may be due to a body wave from a distant storm.

from the long-period array elements of LASA and mathematically rotated vertical signals from ALPA. No attempt was made to correct for instrument response (nominal 25-second resonance). The signals were bandpass filtered using a three-pole Butterworth centered at 20 s (50 mHz). The use of this bandpass, coupled with the response of the array elements, nearly eliminates the double-frequency microseism peak energy from analysis. We should point out that we are using the term 'FK' analysis as a convenience; it is more accurately referred to as frequency-slowness analysis, since we are examining specific frequency planes of the frequency-wave-number power spectrum. The signals were sampled for FK analysis in 39 sequential 128-second windows. Signal time windows were advanced by 100 seconds from previous windows, resulting in window overlaps of 28 seconds. Resulting estimates of approach azimuth and phase velocity were collected and examined for consistency and distribution. We decided to window the data in order to examine the temporal variation in the signal-to-noise ratios and coherency. Windowing the data in this manner also permitted selection of the data on the basis of signal strength and coherency.

Since 20-second period (50 mHz) microseisms are believed to propagate in the form of Rayleigh waves, we anticipated dominant phase velocities between 3 and 4 km/s and so restricted our phase velocity observations to >2.5 km/s. Examining all of the phase velocities, we find that they cluster in the range 3.2 to 3.6 km/s for consistent approach azimuths. Although part of the noise observed on

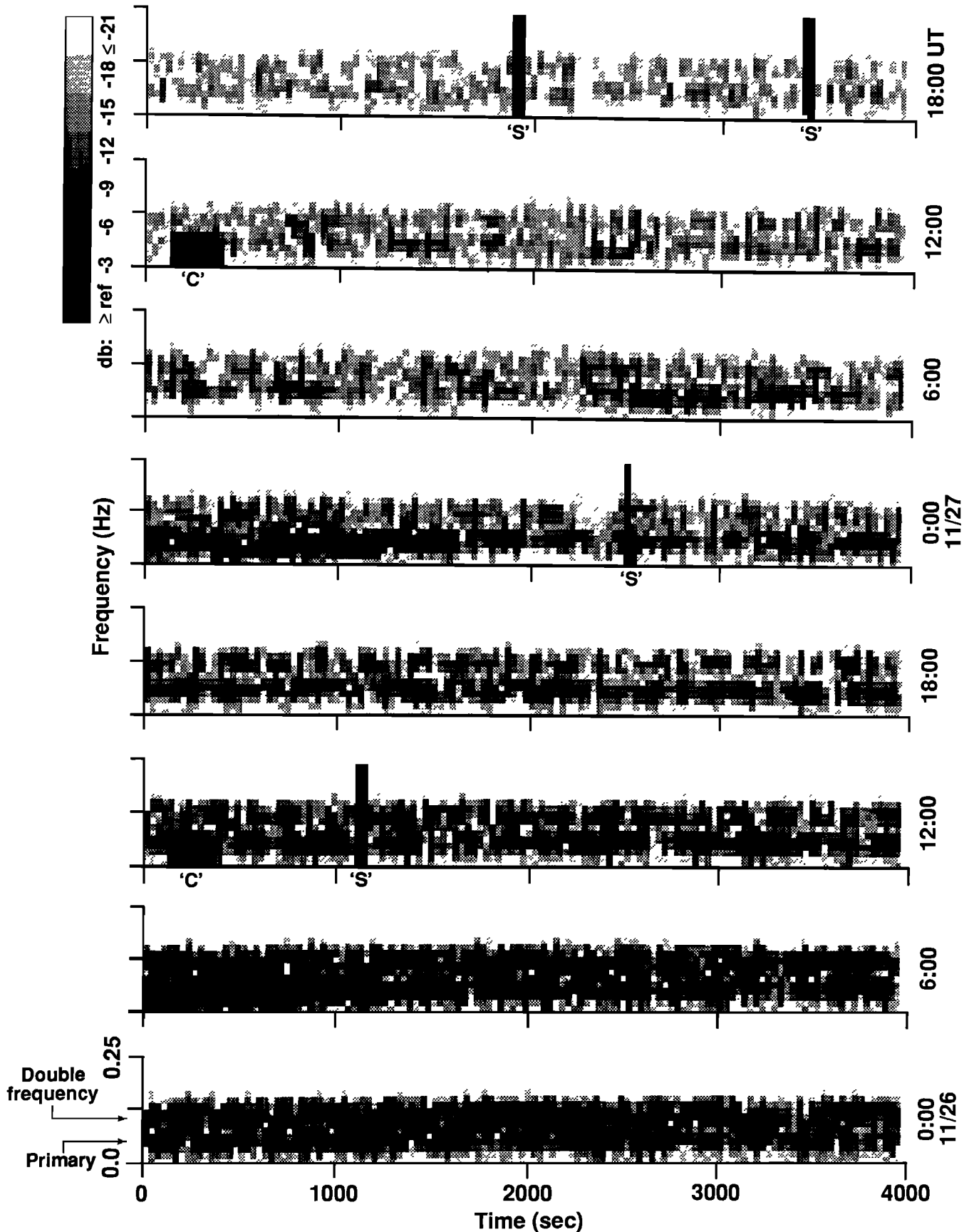


Fig. 4a. Examples of vertical-component spectrograms (time history fast Fourier transform (FFT)) showing the primary- and double-frequency microseism bands associated with concurrent storms in the North Pacific and North Atlantic oceans. Each vertical time band represents a single spectrum obtained with a Parzen-tapered 64-point FFT with frequencies shown from 0 to half Nyquist. Spectra are collected sequentially with 32-point overlaps. Power is relative to an arbitrary reference signal level set constant for the entire figure. Calibration signals recorded with the data are denoted by 'C', and four spurious spikes recorded are denoted by 'S'.

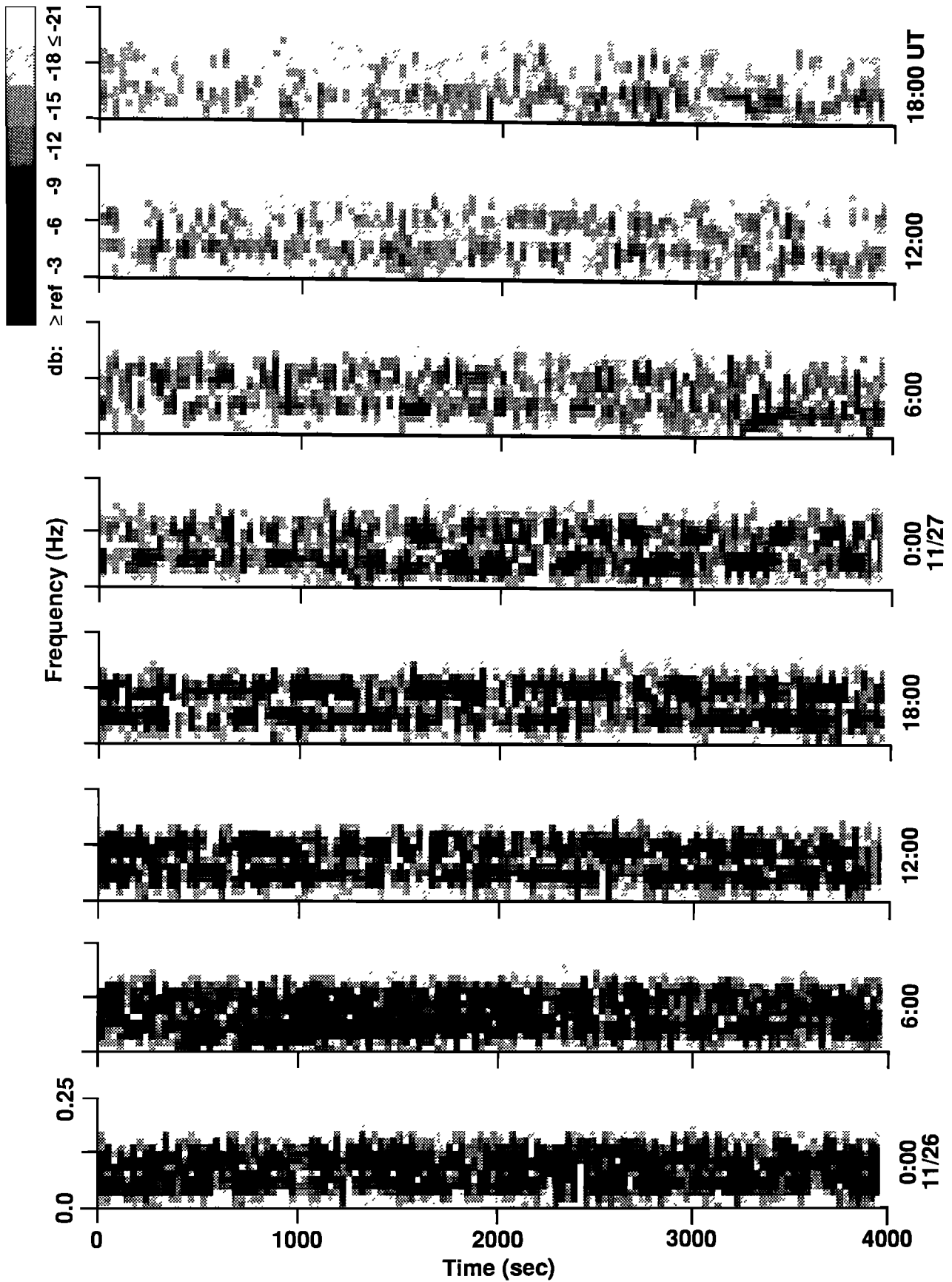


Fig. 4b. Examples of vertical-component spectrograms (time-history fast Fourier transform (FFT)) for LASA showing the primary- and double-frequency microseism bands associated with concurrent storms in the North Pacific and North Atlantic oceans. See Figure 4a caption for details.

land is expected to be locally generated [Sorrells *et al.*, 1971], it is generally incoherent and does not produce significant separable power peaks in the FK analyses. Although FK power peaks associated with the passage of earthquake phases across the arrays were occasionally observed, they were ignored in this context on the basis of their anomalous phase velocities, approach azimuths, spectral signatures, and other characteristics of earthquake phases on the array seismograms. All occurrences of earthquakes that could interfere with the microseisms were confirmed on the International Seismological Centre bulletin which reports the origin times and hypocenters. Data that were selected for this study are confirmed not to be associated with any earthquake activity.

Spectral Analysis

Microseismic signal samples from each array component used in the FK analysis were subjected to spectral analysis. It was expected that variations would be observed in the spectral character of the microseisms, since their signatures are known to vary with the storm intensity [e.g., Korhonen and Pirhonen, 1976]. We found an order of magnitude fluctuation in the primary microseism signal on a time scale of minutes as shown in Figure 4, an example of a vertical spectrogram (time-history spectra plot) for the period November 26-27, 1973. The existence of simultaneous storms in the Atlantic and Pacific oceans implies that the signal spectrum observed at either array represents a composite of the spectral characteristics of their associated microseism signal sources.

We compared microseism spectra obtained during two separate time windows manifesting FK power peaks at azimuths consistent with the known locations of the Atlantic and Pacific storms. Figure 5 gives two examples of the vertical spectra obtained by averaging over all usable array elements for separate time periods when the dominant FK power spectra peaks alternated between the two storms. The typical spectrum obtained while the Atlantic storm microseism dominated the FK power distribution exhibits a markedly higher primary microseism peak frequency than the corresponding spectrum obtained while the Pacific storm was dominant. During the times when the peak FK power appears to be associated with the Pacific storm, the spectra exhibit an inflection at the peak power frequency of the Atlantic storm (Figure 5). The reverse is true when the peak FK power is associated with the Pacific storm. Our current FK analysis routine reports only the azimuth and phase velocity for the maximum FK power peak. Secondary FK power peaks are clearly resolvable and will be examined in future work.

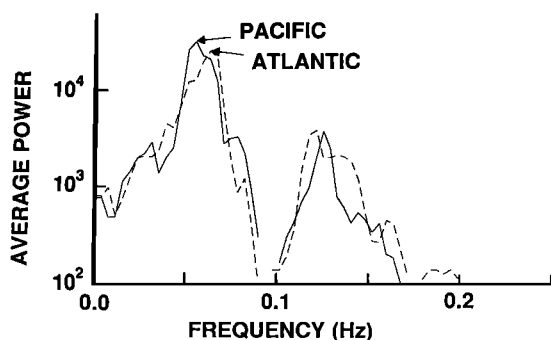


Fig. 5. An example of uncorrected array-averaged vertical spectra for time periods when Atlantic storm (dashed curve) and Pacific storm (solid curve) microseisms dominate the FK power spectrum. Note slight differences in spectral power distribution.

RESULTS AND DISCUSSION

Primary microseism spectral power is observed to vary by more than an order of magnitude over a time scale of minutes. When signals from multiple microseismic sources are recorded by an array, their separate source amplitude fluctuations are observed as the modulation of their corresponding FK power peaks. Since the microseismic signal amplitudes from the two storms of this study were nearly equal, a moving window analysis provided representative azimuth determinations. The relative stability of individually determined approach azimuths is displayed as a histogram in Figure 6. A similar distribution is also exhibited in phase velocities, ranging from 3.2 to 3.6 km/s, being characteristic of Rayleigh mode propagation over continental paths. Although the FK peak observations accurately reflect the significant microseismic sources active during each window, we wish to emphasize that the number of observations made for a given azimuth are skewed in the sense that the stable subordinate peaks associated with temporarily weaker microseismic sources are not well represented by our current analysis scheme.

Figure 7 shows the microseism source locations determined by triangulation of the approach azimuths. The distribution of approach azimuths determined for different time windows for the same 4000-point data sample provides an estimate of the azimuth stability and

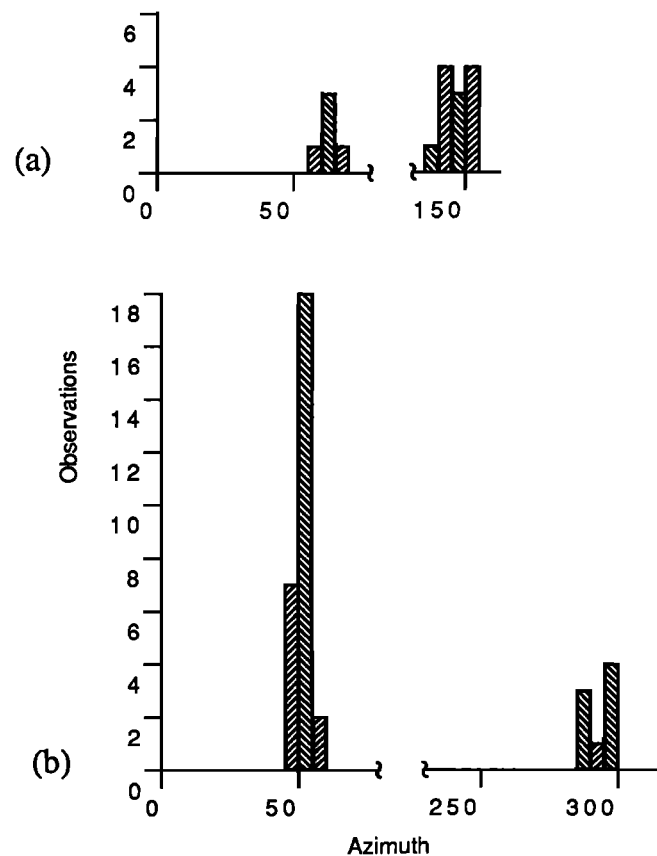


Fig. 6. Histogram showing an example of the distribution of consistent approach azimuths determined from FK analyses of (a) ALPA and (b) LASA microseism data. Anomalous azimuth and phase velocity determinations, based on the whole time period analyzed, have been deleted for clarity. We discarded azimuths associated with (1) phase velocities outside the typical 3.4-3.6 km/s and (2) with low S/N (see text). The two azimuth peaks shown in each graph are associated with the two separate microseism sources discussed in the text. The azimuth distributions are used to estimate the likely microseismic source locations shown in Figure 7.

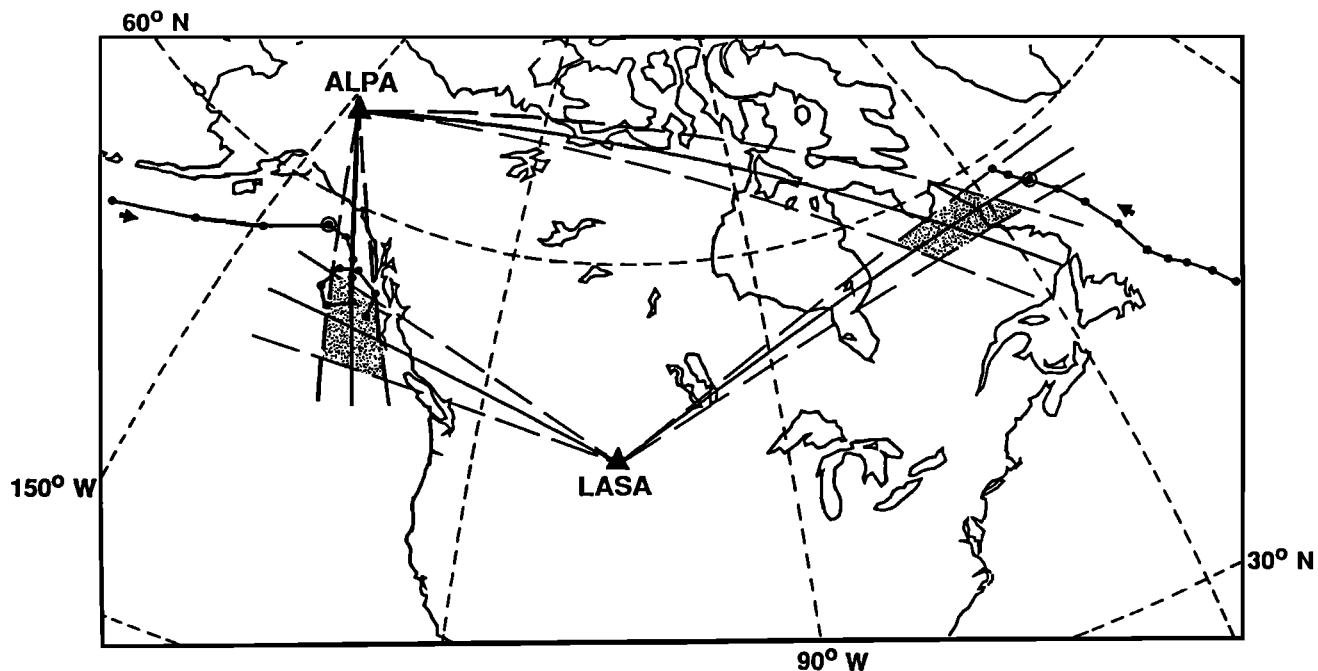


Fig. 7. Map showing locations and tracks of the centers of the two major storms believed to be the source of the microseisms analyzed in this study [after *Mariners Weather Log*, 1973]. The storm center locations are indicated by solid circles at 6-hour intervals. Two small reference arrows are placed at the reported storm positions for November 25, 1800 UT and indicate storm trajectories. The two solid dots enclosed by open circles show the storms' positions on November 26, 1973 at 1200 UT. The azimuths determined from multiply windowed FK analyses for the 4000-second sample starting at this time and their estimated standard deviations are indicated by solid and dashed lines, respectively. The shaded areas give an estimate of the areas most likely to contain the microseism sources. The perimeters of the shaded areas are drawn from the standard deviations of the FK-determined azimuth distribution over the length of the time sample (4000 seconds). Locations of ALPA and LASA arrays are denoted by solid triangles. This map is an azimuthal equidistant projection centered on the midpoint of a great circle connecting the two arrays.

error. For the Atlantic storm, the azimuths obtained from LASA differ by 4° over a 48-hour period (i.e., eight separate 4000-second data samples), while the approach azimuths determined from ALPA data are nearly constant. The approach azimuth variation for the Pacific storm is similar: LASA azimuths differ by 16° , while the azimuths from ALPA are within 3° over the same time period. The difference in azimuth distribution reflects the resolution difference of the two arrays, but also suggests the approach azimuth stability. Examples of the approach azimuth distributions are shown in Figure 6 for both ALPA and LASA obtained from one 4000-second sample starting at 1200 UT, November 26, 1973. For clarity, only the dominant approach azimuth distributions are shown. Examining the clustering of azimuths determined for the entire time period studied suggests a stable location for the dominant FK power peaks.

When both storm microseism source amplitudes were low, other FK power peaks appeared with more random azimuthal distribution. These may be ascribed to local or distant sources but could not be triangulated because of insufficient FK peak power at either array. The mean azimuths determined from the remaining multiply windowed FK analyses, for a concurrent 4000-second sample from each array, are indicated by solid lines in Figure 7. The intersections of standard deviations in the mean approach azimuths (dashed lines) are used to construct the perimeters of the shaded source areas shown in Figure 7. It appears that the microseism source location associated with the Pacific storm is near the west coast of the Queen Charlotte Islands, where the average water depth is 3000-4000 m. The location for the Atlantic storm source is more strongly associated with the coast, occurring near the coastline of Newfoundland as shown in Figure 7. For the Pacific storm, however, the actual storm posi-

tion is well to the northwest of the array-detected locations. Also, the triangulation microseism source locations determined for the time periods corresponding to earlier synoptic positions of the same storm do not track the fast-moving Pacific storm, but remain rather stable near the position shown in Figure 7. The persistent location of the microseismic source suggests that it is not a direct function of the storm position. We speculate, instead, that it is associated with a stable near-coastal "bright" spot that acts to enhance the coherent storm-generated microseismic energy received at the two arrays.

Although pelagic storms provide the source of microseismic wave energy, it is the interplay between the storm parameters, the resulting storm waves, the direction of storm wave propagation, and the nearshore processes that acts to enhance or inhibit the production of coherent single-frequency microseisms. From the perspective of a seismic array, over a specific time interval, only the most energetic and coherent portion of the noise field is detected in the FK domain. FK analysis is sensitive to, and therefore reflects the position of, only a fraction of the total storm-related microseismic noise field.

The results of this study demonstrate the capability of FK analysis to identify two or more concurrent sources of coherent microseism energy. The stability and robustness shown by the method permit simultaneous determination of phase velocities and approach direction of the microseismic wave propagation. Triangulation by two arrays reveals the locations of two microseism sources which appear to be clearly associated with storm systems but not as a close function of their locations.

Some interesting questions have emerged from the results of this study. In particular: what makes a particular shoreline or nearshore location bright in an FK power sense? We speculate that it is likely

to be the result of some subtle combination of local coastal resonance modes involving coastal sea bottom morphology, storm wave spectral characteristics and approach directions. Do similar storms excite the same local modes? In other words, are there particular nearshore environments that would preferentially tend to generate FK peaks regardless of the storm location within a given oceanic basin? Does the excited nearshore region vary with storm speed, peak frequency, or tracking direction? A related, but still unanswered, question regards the source location of double-frequency microseisms. Does its location exhibit similar stability? We expect to report on these and related questions in the course of our ongoing research.

CONCLUSIONS

We have analyzed 20-second microseisms recorded simultaneously on two land-based long-period arrays (ALPA and LASA) during November 1973. We apply running-window frequency-wave number analysis to extract approach azimuths from bandpass-filtered one-hour samples of the microseismic noise field recorded by the two arrays. Microseismic source azimuths exhibit sufficient stability over periods of one hour to permit determination of reliable source locations by triangulation with the two arrays. Locations for two microseism noise sources associated with two separate Atlantic and Pacific storms were found simultaneously with these methods. In both cases, we find that the strongest coherent microseismic noise sources are associated with near-coastal locations that do not appear to be a close function of storm position. We speculate that these near-coastal locations are, in some sense, preferentially excited by ocean storm waves arriving from distant atmospheric disturbances. The excitation may result from some combination of constructive interference of coastal waves and their reflection, an effect of local ocean bottom morphology on ocean wave parameters, and the coastline shape. We emphasize that, although entire coastlines may be illuminated by storm waves giving rise to microseisms at this frequency, the method of simultaneous FK analysis and triangulation is primarily sensitive to the strongest microseismic signal coherencies recorded during a given time span.

Acknowledgments. We wish to thank Randy Jacobson for helpful discussions during the course of this work. Tom McElfresh was instrumental in the development of the software required to retrieve these data. We are grateful to John Woolson for his help in sorting out the complexities associated with dearchiving the data. We thank Margaret Marshall and Robert Wagner for their careful and patient assistance in retrieving and analyzing these data. This work was supported by ONR contract N00014-88C-0035.

REFERENCES

- Capon, J., High resolution frequency-wavenumber spectrum analysis, *Proc. IEEE*, 57, 1408-1418, 1969.
- Capon, J., Analysis of Rayleigh-wave multipath propagation at LASA, *Bull. Seismol. Soc. Am.*, 60, 1701-1731, 1970.
- Darbyshire, J., Identification of microseismic activity with sea waves, *Proc. R. Soc. London., Ser. A*, 202, 439-448, 1950.
- Darbyshire, J., and E. O. Okeke, A study of primary and secondary microseisms recorded in Anglesey, *Geophys. J. R. Astron. Soc.*, 17, 63-92, 1969.
- Forbes, C. B., R. Oberchain, and R. J. Swain, The LASA sensing system design, installation and operation, *Proc. IEEE*, 53, 1834-1843, 1965.
- Geotech, Project VT/8707 Alaskan Long-Period Array, *Final Report AFTAC F33657-69-C-0273*, Teledyne Geotech, Alexandria, Virginia, 1970.
- Hasselmann, K., A statistical analysis of the generation of micro-seism, *Rev. Geophys.*, 1, 177-210, 1963.
- Haubrich, R. A., and K. McCamy, Microseisms: Coastal and pelagic sources, *Rev. Geophys.*, 7, 539-571, 1969.
- Haubrich, R. A., W. H. Munk, and F. E. Snodgrass, Comparative spectra of microseisms and swell, *Bull. Seismol. Soc. Am.*, 53, 27-37, 1963.
- Iyer, H. M., A study of direction of arrival of microseisms at Kew Observatory, *Geophys. J.*, 1, 32-43, 1958.
- Korhonen, H., and S. E. Pirhonen, Spectral properties and source areas of storm microseisms at NORSAR, *Sci. Rep. 2-75/76*, Teledyne Geotech, Alexandria, Virginia, 1976.
- Lacoss, R. T., E. J. Kelly, and M. N. Toksöz, Estimation of seismic noise structure using arrays, *Geophysics*, 34, 21-38, 1969.
- Longuet-Higgins, M. S., A theory of the origin of microseisms, *Phil. Trans. R. Soc. London*, 243, 1-35, 1950.
- Mack, H., Spatial coherence of surface waves, *Seismic Array Analysis Center Rep. 8*, Teledyne Geotech, Alexandria, Virginia, 1972.
- Mariners Weather Log, U. S. Dept. of Commerce, NOAA, Natl. Environ. Satellite, Data and Information Service (U. S. Govt. Print. Office), Washington, D.C., 1970-1973.
- Oliver, J., A worldwide storm of microseisms with periods of about 27 seconds, *Bull. Seismol. Soc. Am.*, 52, 507-517, 1962.
- Rind, D. H., and W. L. Donn, Microseisms at Palisades, 2, Rayleigh wave and Love wave characteristics and the geologic control of propagation, *J. Geophys. Res.*, 84, 5632-5642, 1979.
- Sorells, G. G., J. A. McDonald, Z. A. Der, and E. Herrin, Earth motion caused by local atmospheric pressure changes, *Geophys. J. R. Astron. Soc.*, 26, 83-98, 1971.
- Toksöz, M. N., and R. T. Lacoss, Microseisms: Mode structure and sources, *Science*, 159, 872-873, 1968.

R. K. Cessaro and W. W. Chan, Teledyne Geotech Alexandria Laboratory, 314 Montgomery Street, Alexandria, VA 22314.

(Received November 8, 1988;
revised May 25, 1989;
accepted May 25, 1989.)